Performance Characteristics of an Aerospace Nickel Hydrogen Cell- Experimental Data and Theoretical Predictions

B. V. Ratnakumar, P. Timmerman, D. Perrone and S. Di Stefano
Electrochemical Technologies Group, Jet propulsion Laboratory, Pasadena, California 91109

ABSTRACT

Experimental data have been generated on an Eagle-Picher *50* Ah, IPV Ni-H_2 cell under various experimental conditions These conditions included discharges and charges at different currents and temperatures, in order to determine the effect of these on the charge and discharge efficiencies of the Ni-H_2. Such a database, hither to not available in the literature, should provide considerable support to the modeling effort in terms of identifying appropriate values for the model parameters '1 he charge behavior points to an interesting possibility of examining the multiple phases of the positive electrode active material 'These studies have been augmented by the simulations from our mathematical model,

1.0 Introduction

Prediction of battery performance through simulated tests using appropriate mathematical models would provide useful guidelines for a proper management of a power subsystem on a spacecraft. JPL has been involved for the past few years in the development of mathematical models for aerospace scaled nickel-cadmium and nickel-hydrogen rechargeable cells[1] The earlier versions have been built around the (porous electrode) cell models developed at '1 exas A & M University[2], utilizing the macrohomogeneous approach of Newman, [3] Various aspects addressed in the cell model include : 1) material balance for the dissolved species generated/consumed by the electrochemical reaction and transported by diffusion and migration, 2) variations in the electrolyte porosity due to differences in the molar volume of the reactants and products, 3) changes in the electrochemical potential in the solid phase and in the electrolyte, *4)* charge transfer kinetics through a modified Butler-Volmer rate equation, 5) principles of conservation of charge in the electrochemical cell, and *6)* effects of intercalation and slow diffusion of protons into the positive electrode. The recent models developed in conjunction with the Univ. South Carolina are based on the assumption of a homogeneous reaction rate (as in a planar electrode), which is justified by a relatively insignificant effect of the mass transfer processes in the electrolyte phase. Some of the improvements made at JPL in translating the basic cell model into a useful battery engineering tool include 1) a translator routine, i.e., a design routine containing the electrode/cell manufacturer's design details to permit simulation of any cell 2) a charge definition routine containing operational data Jilts which allow the implementation of any discharge and/or charge protocol, and 3) allowance for multi-cell configurations in the model in order to predict the thermal and electrical characteristics of a Ni-H_2 battery[4] Furthermore, the recent model takes into account the existence of two phases of positive active material, i.e., β and γ forms of NiOOH and the corresponding reduced forms, β and α-$Ni(OH)_2$, for a more accurate prediction of the discharge and charge behavior.[5] The model thus permits discharge/charge of any given cell under any specified test conditions, such as at constant current, constant voltage or constant power, with limits of either time, vohagc/current or temperature.

in order to verify the capability of the above battery model to predict the performance under various test conditions, such as at different charge and discharge currents and at temperatures, experimental studies have been made. on an IPV SO Ah Ni-H_2 cell. Here, we present some of the experimental data with the IPV 50 Ah cell under various test conditions outlined below. Also, the cell behavior is predicted under similar conditions using the

above mathematical model for a comprison with the experimental data.

2.0 : Cell Design Details

The Ni-H_2 cell for the experimental studies was supplied by Eagle Picher Inc , Joplin, Missouri. The cell was built on 'rabbit ear, mantel' design and contains 40 positive (NiOOH) and negative (hydrogen) electrodes. The nickel electrodes were made with sintered (from slurry) Ni plaques into which the active material was incorporated by aqueous electrochemical impregnation process 10 total thickness of 0.03". The hydrogen electrodes are standard flight-type electrocatalytic gas-diffusion membrane electrodes of 0.005" nominal thickness. The separator is standard Zircar in two layers. The cell is stacked in back-to-back arrangement. The gas screens are non-woven polypropylene of 0.024" thickness. The cell is equipped with a strain gauge for monitoring the changes in internal pressure. After normal activation, conditioning and ATP (Acceptance Test Procedure) testing, the cell was in storage for about two years, before the present tests at JPL.

3.0: Test Protocol

One of the objectives of the present experimental study is to generate data base on the performance of Ni-H_2 cell under various test conditions for a comparison with the simulations and thus a validation of the model, Such data are not available in the literature. For example, it is essential to separate the charge and discharge efficiencies at various rates and temperatures If the charges and discharges are carried out at the same temperatures, as has been done in the literature, it is hard to separate the inefficiencies setting in during charge from those occurring in the subsequent discharge. "1 he test protocol chosen for this study therefore constitutes charges at various temperatures and rates followed by discharges under standard conditions (C/2 at 10 °C) and discharges at various rates and temperatures after charges under standard conditions (C/10 @ 10 "C).

4.0: Performance characteristics : Experimental vs. Simulations

4.1 Discharge Behavior

Fig. 1 illustrates the typical discharge behavior of the SO Ah Ni-H_2 cell al *2 h* (C/2) rate, at 10 °C. The cel I voltage drops rather sharply in the initial stage of discharge arid levels off later on, around 1.25 V. The cell pressure falls linearly during the discharge from an initial value of- 750 psi to about 75 psi.

The simulated discharge behavior under these conditions is shown by the dashed line in Fig.1. As may be seen from the figure, there is an excellent agreement between the measured and predicted discharge potentials. In order to achieve as good an accuracy in the predictions, it is required to incorporate a mul(i-phase reaction mechanism for the positive electrode. It is well known that nickel oxyhydroxide exists in two phases, i.e., β-NiOOH and γ-NiOOH. The former is the conventional, more stable form, whereas the latter forms essentially during overcharge. '1 he reversible potentials of these phase are about 60 mV apart,[6,7] which results in sloping discharge curves in the initial stages. For the above simulations, the proportion of the γ-phase is ~ 90% and the reduction kinetics of the γ-NiOOH are marginally slow (1.0 X 10^{-4} as compared to ?.0 x 1()-4 A/cm^2 for the β-NiOOH) but the diffusional kinetics and the ohmic effects are identical for both the phases.

4.2 Charge Characteristics

The typical charge behavior of the Ni-H_2 cell is illustrated in Fig. ?. Once again, the pressure increases lineally in the course of charge and levels off al the end of charge, i.e., during oxygen evolution and recombination, as evident from the voltage profile The simulated charge behavior is shown by the dashed line in Fig. 2. Once again, there is a good agreement between the predicted and the observed charge voltages, especially in the initial portions of charge, which was found to be difficult to obtain with single phase of nickel oxyhydroxide couple. In the latter stages of charge, i .e., during overcharge, however, there is some divergence in the predicted and observed voltages. This is attributed to the fact that the simulations were carried out under isothermal conditions. Since the]oll-over in the cell voltage is related to the exothermicity of the oxygen

evolution/recombination process, it can be appropriately modeled by incorporating gas-side thermal model as developed earlier for Ni-Cd[4]. The development of similar model for the present Ni-H_2 cell is underway.

4.3 Discharge at Different Rates

The discharge behavior of the Ni-H_2 cell as a function of discharge rate, at 10°C following charges under similar conditions, i.e., C/10 for 16 h at 10 °C, is shown in Fig. 3A. The discharge curves show little change upon changing the rate from 5 A (C/10) to 25 A (C/2). The capacity drops by ~4% from the lowest to the highest rate studies. Such curves were generated both 10 °C and 20 °C. Interestingly, the capacity is rather low at low drains (C/10 *or 5 A)* in the latter case (Fig. 3B), which is attributed to the self discharge occurring at comparable rate. In separate tests, the cell was found to lose about 15% over 10 days at 10 °C compared to ~28% in 5 days at 20 °C.

The simulated discharge curves also indicate similar effect on the discharge current. The only significant difference is that the capacity loss at low rates is not as prominent as in the experimental data (Fig. 3B). This is due to the fact that the present model doesn't take into account the self-discharge of the cell, occurring in background, which is being implemented now.

4.4 Discharge at Different Temperatures

The effect of the discharge temperature on the discharge behavior of the Ni-H_2 is illustrated in Figs. 4. The charges preceding these discharges were carried out under identical conditions, i.e., at C/10 for 16 hours at 10 °C, and the discharges at C/5 at the selected temperature. The simulated discharge curves at various temperatures are shown in Fig. 4B. These simulations were carried out by using an appropriate set of values for the temperature coefficients of various model parameters, such as exchanges currents, electrolyte and electrode conductivities and diffusion coefficients, as done earlier for Ni-Cd[4]. As may be seen from Figs 4A & 4B there is a fairly good agreement between the predicted and observed discharge behavior at different temperatures. The simulated discharge capcity, is, however, lower than the experimental values

4.5 Charge at Different Rates

In order to examine the charge efficiency of the Ni-H_2 cell at various charge rates, charging of the cell has been carried out at different rates, followed by discharges under similar conditions, i.e., at C/2 at 10 °C. Fig. 5 shows the charge curves at various rates, i.e., at 020, C/10, C/5, C/2 and C. At the highest rate studied (C rate), the cell wasn't completely charged due to the imposed limits on the charge voltage and cell pressure. Interestingly, in the corresponding discharge curves, the sloping portion is not as prominent. The simulated charge curves as a function of rate are shown in Fig. 5B. The charge efficiency has been calculated based on the capacities in the subsequent discharges (Fig. 5C). It may be seen from Fig. 5C that the charging process is more efficient at high rates., which may be attributed to the improved current efficiency for the charging of the $Ni(OH)_2$ electrode at high rates.

4.6. Charge at Different Temperatures

The efficiency in charging of the Ni-H_2 cell at various temperatures has been determined from a series of charges at various selected temperatures, and from subsequent discharges under similar conditions, i.e., at C/2 at 10 °C. Fig. 6 shows the charge curves at various temperatures, i.e., at -20, -10, 0, 10, 20 and 35 °C. As may be seen from the figure, the charge voltage increases with a decrease in the temperature. Interestingly, the roll-over becomes more prominent at low temperatures, which may be related to the exothermicity of oxygen evolution/ recombination processes. Furthermore, there is a distinct second plateau in the charge voltage before the roll-over due to oxygen evolution. This may be ascribed to the electrochemical conversion of β-$Ni(OH)_2$ to γ-$Ni(OH)_2$. Once again, using appropriate temperature coefficients for the temperature coefficients for the kinetics processes, such as exchange current densities, electrolyte/electrode resistivities and diffusion coefficients, we are able to simulate this behavior in a Ni-H_2 cell (Fig. 6B). The efficiency in the charging of the Ni-H_2 cell is calculated from the subsequent discharges (Fig. 6C). It is evident from the figure that the charging process becomes efficient at temperatures below 10 °C. At higher

temperatures, the efficiency drops rather sharply, due to the parasitic oxygen evolution at the $Ni(OH)_2$ electrode.

5.0 Conclusions

Useful database on the performance characteristics of a Ni-H_2 cell has been generated, using a 50 Ah IPV cell of Eagle-Picher, Inc. The results indicate the optimum ranges of discharge/charge currents and temperatures and provide a support to the on-going mathematical modeling activity in terms of choosing appropriate values for the model parameters. Reasonably good agreement has been observed between the experimental data and simulation from the mathematical model for Ni-H_2 cell. The charging behavior at low temperatures reveals the possibility of electrochemical conversion of β-NiOOH into the corresponding γ-form before the onset of oxygen evolution/recombination, as demonstrated by the simulations. Further basic electrochemical studies are underway to verify this mechanism.

6.0: Acknowledgments

This work was carried out at the Jet Propulsion Laboratory, California Institute of Technology, under contract with the National Aeronautics and Space Administration and was sponsored by NASA Chief Engineer's Office. We thank Drs. Chris Fox and Dwaine Coates of Eagle Picher Inc., Joplin, MI for providing their Ni-H_2 cell for these studies.

7.0: References

1. P. J. Timmerman, *Proc. 29th IECEC*, 112, (1994); P. J. Timmerman, S. DiStefano, P. R. Gluck and D. E. Perrone, *Proc 26th IECEC*, 358 (1991); K. Clark, G. Halpert and P. Timmerman, *24th IECEC*, 1479 (1989); P. Timmerman, K. Clark and G. Halpert, *Proc. 23rd IECEC*, (1988).
2. J. Newman and W. H. Tiedemann, *AIChE Journal*, 21,25 (19-/s); J. Newman, *Ind and Eng. Chem. Fund.*, 367-369 (1978).
3. D. Fan and R. E. White, *J. Electrochem. Soc.*, 138), 17 (1991); *J. Electrochem. Soc.*, 138, 2952 (1991); Z. Mao and R. E. White, *J. Electrochem. Soc.*, 138, 3354 (1991),; Z. Mao, P. De Vidts, R. White and J. Newman, *J. Electrochem. Soc.*, 141, 54 (1994); P. De Vidts and R. E. White, *J. Electrochem. Soc.*, 142, 1509 (1995).
4. B. V. Ratnakumar, P. Timmerman, C. Sanchez, S. Di Stefano and G. Halpert, *J. Electrochem Soc.*, 143 pp. 00 (1996).
5. P. J. Timmerman and B. V. Ratnakumar, *Space Power Conf.* at Albuquerque, NM, April 17-20, 1998.
6. H. J. Bode, K. Dehmelt and J. Witte, *Electrochim. Acta*, 11, 1079 (1966).
7. R. A. Huggins, H. Prinz, M. Wohlfahrt Meherens, L. Jorissen and W. Witschel, *Solid State Ionics*, 70/71, 417 (1994).

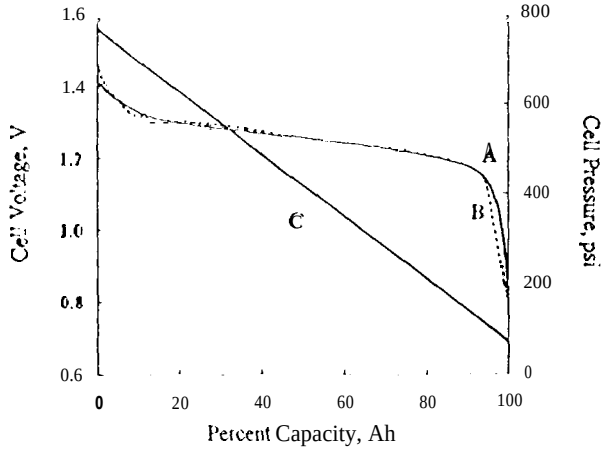

Fig. 1: A) Simulated and B) Experimental discharge curves of a Ni-112 cell at C/2 and 10°C. Curve C denotes the experimental cell pressure during discharge.

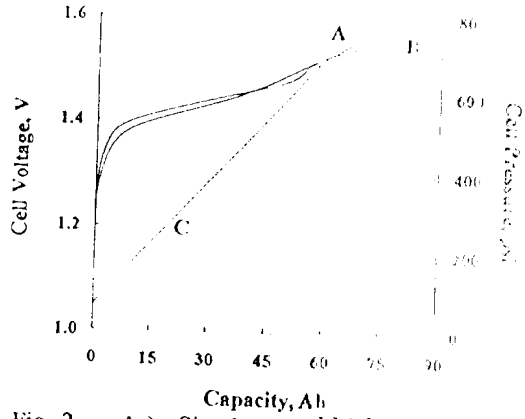

Fig. 2 : A) Simulated and B) Experimental charge curves of a Ni-H_2 cell at C/2 and 10°C. Curve C denotes the experimental cell pressure during charge.

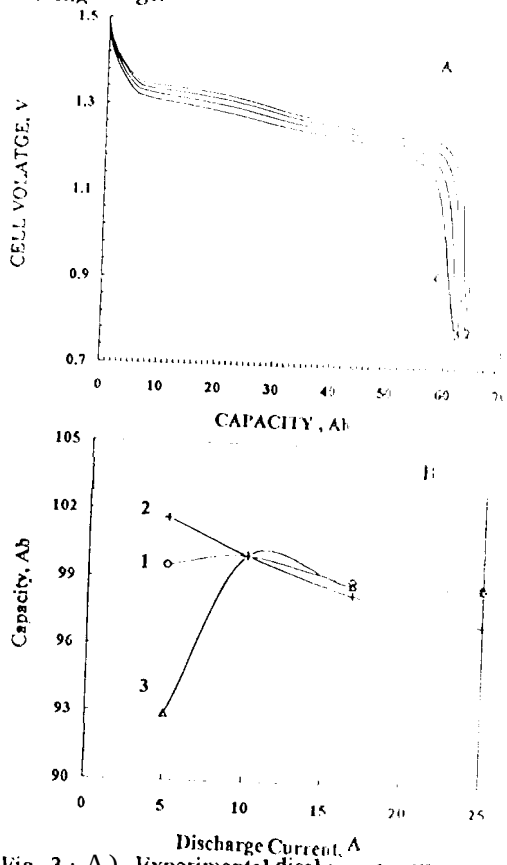

Fig. 3 : A) Experimental discharge curves of a Ni-H_2 cell at various rates of 1) C/10, 2) C/5, 3) C/3 and 4) C/2 and 10°C, after charges at C/10 at 10 °C. Chart B shows the variation of 1) simulated discharge capacity at 20°C and experimental capacity as a function of rate at 2) 10°C and 3) 20°C, respectively.

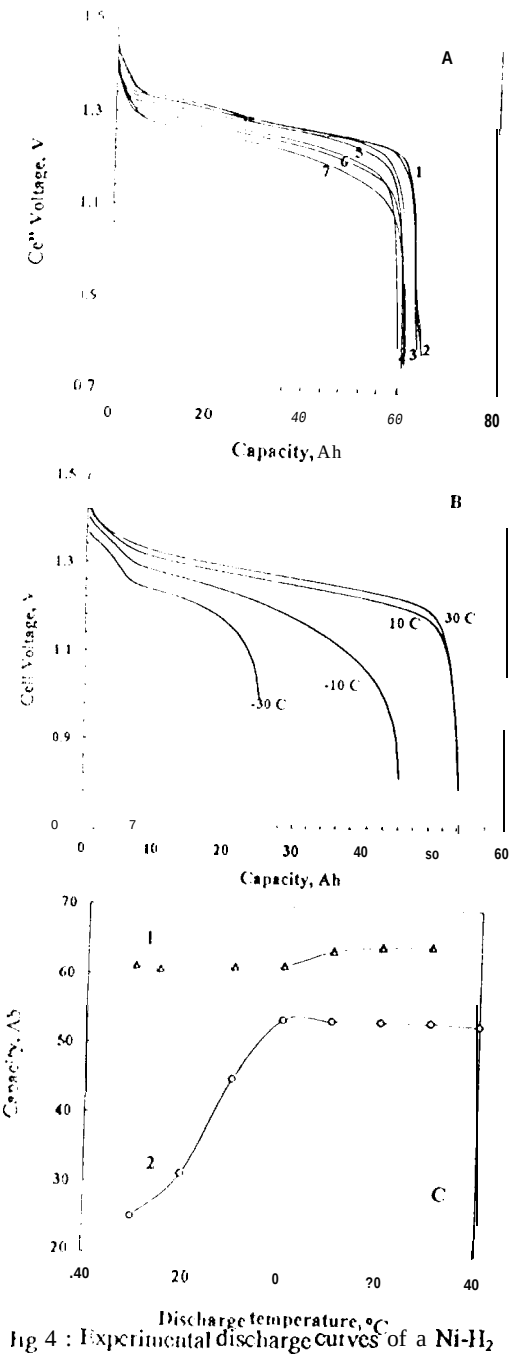

Fig 4 : Experimental discharge curves of a Ni-H_2 cell at C/5, after charges at C/10 and 10°C, at various discharge temperatures of 1) 30, 2) 20, 3) 10, 4) 0, 5) -10, 6) -20 and 7) -30 °C, respectively. Fig B denotes similar curves from the model and Fig C shows the variation of 1) experimental and 2) simulated discharge capacity with temperature